NEGATIVE PARTICLE PRODUCTION AT THE 70 GeV IHEP ACCELERATOR

Yu.B. Bushnin, S.P. Denïsov, S.V. Donskov, A.F. Dunaitsev, Yu.P. Gorin, V.A. Kachanov, Yu.S. Khodirev, V.I. Kotov, V.M. Kutyin, A.I. Petrukhin, Yu.D. Prokoshkin, E.A. Razuvaev, R.S. Shuvalov and D.A. Stoyanova,

Institute for High-Energy Physics, Serpukhov, USSR.

J.V. Allaby, F. Binon, A.N. Diddens, P. Duteil, G. Giacomelli[††], R. Meunier[†††], J.-P. Peigneux[**], K. Schlüpmann, M. Spighel[*], C.A. Ståhlbrandt, J.-P. Stroot[*†] and A.M. Wetherell,

CERN, Geneva, Switzerland.

ABSTRACT

Data are presented on the yields of π^-, K^-, and $\bar{p}$ produced at small angles by 70 GeV proton-aluminium interactions. The momenta of the secondaries studied were greater than 40 GeV/c. Upper limits have been obtained on the production of antideuterons and possible new particles up to a mass of 2.2 GeV in this new energy region.

* * *

To be submitted to Physics Letters

February 1969

---

†) Visitor from Institut Interuniversitaire des Sciences Nucléaires, Bruxelles.

††) Visitor from Istituto Nazionale di Fisica Nucleare, Bologna.

†††) Visitor from CEN, Saclay.

*) Visitor from Institut de Physique Nucléaire, Faculté des Sciences, Orsay.

**) Visitor from Université de Clermont-Ferrand.

This letter presents experimental results on the negative particle fluxes produced by 70 GeV protons bombarding aluminium targets in the IHEP proton synchrotron. The data were taken at small laboratory production angles ($\theta < 15$ mrad) and secondary momenta greater than 40 GeV/c. Some additional data were taken at incident energies of 20 and 43 GeV.

Experiments[1] at lower incident energies have been carried out at many laboratories. The motivation of this experiment was the need for information on the beams of particles which could be obtained from the IHEP 70 GeV accelerator and on the techniques necessary to identify the particles, as well as the desire to understand more clearly the physics of particle production at high energies.

During the experiment, the proton synchrotron accelerated an average beam of 3×10^{11} protons every 7 seconds at 70 GeV (5 sec at 20 GeV). The beam spill was approximately constant over a time of 0.4 sec. The secondary beam channel was designed to accept negative particles of 40, 50, or 60 GeV/c produced at an angle of 0 mrad from one of three targets spaced azimuthally inside a magnet unit of the accelerator. By varying the radial position of these targets, various combinations of momentum and angle could be obtained in the range 40-60 GeV/c and 0-15 mrad. The production angle and momenta of the secondaries from any one target could not be independently varied. Some additional data were taken at momenta greater than 60 GeV/c in a slightly modified version of this beam. The targets were made of aluminium, and were cylindrical with length 21 mm and diameter 2 mm. Two independent monitors, a threefold telescope P and a fourfold telescope F, were aligned on the target to detect charged secondaries.

Figure 1 shows the beam layout. Collimators K_1 and K_2 defined the beam acceptance vertically and horizontally, respectively. The quadrupole lenses L_1- L_4 produced a horizontal focus at the momentum slit K_3 which defined the momentum acceptance; L_5- L_7 produced the parallel part (between L_7 and L_8) and L_9- L_{10} yielded a final focus in both horizontal and vertical planes at the position of counter S_5. The main magnetic analysis was performed by the

magnetic field of the synchrotron and the bending magnet M_1. At K_3 the momentum dispersion was 1% per 6 mm. The purpose of magnets M_2, M_3 was to cancel the momentum dispersion in angle in the parallel part containing the differential Čerenkov counters, and to provide an achromatic focus at S_5. The total beam length to S_5 was 120 m.

The composition of the beam was measured independently by various combinations of Čerenkov counters of different design, in order to gain information on possible difficulties of detection in this new momentum range. This redundancy provided a valuable cross-check of the data. The beam was defined geometrically by scintillation counters A_2A_3 or $S_2S_3S_4$ S_5. For particle identification the following detectors were available: two chromatically compensated differential Čerenkov counters, D and Δ (DISC's); two Čerenkov counters C_1 and C_2, which could be used as either threshold or differential-threshold counters; a final threshold Čerenkov counter C_3, which was frequently used in anticoincidence. Their positions are indicated in Fig. 1. The D counter was 2 m long and used CO_2 gas as radiator[2]. The Čerenkov light from the desired particles, after passing through a compensator for chromatism, was detected by nine photomultipliers placed behind a variable aperture annular diaphragm. Two logical combinations of the photomultiplier output pulses were used throughout the experiment, labelled D_6 and D_9, respectively. D_6 consisted of a sixfold coincidence between three pairs of phototubes and three single phototubes. D_9 was a direct ninefold coincidence which gave the best signal-to-noise ratio, but rather small efficiency ($\approx$ 35% with smallest diaphragm opening), resulting from low photoelectron statistics[3]. The efficiency of D_6 was $\approx$ 70%. The Δ counter was 2.5 m long and similar in construction to the D counter. However, it had 12 photomultipliers to detect the Čerenkov light, but with logic very similar to the D counter, enabling an equivalent choice of the order of coincidence demanded. Normally the combination Δ_6 was used with an efficiency in the range of 35 to 70%. Both counters had a resolution of $\Delta\beta \approx 2 \times 10^{-5}$. The refractive index of the gas of both counters was measured with Rayleigh interferometers, one using

a visual setting on the achromatic fringe and a visual read-out of the micrometer driving the compensating glass plate, the other using a digital output of the number of fringes obtained in filling the empty refractometer to the counter pressure, using the monochromatic red line of a He - Ne laser. An absolute measurement of the particle velocity was obtained through an almost linear relationship between particle velocity and number of fringes, where the constants were all measurable quantities. Hence, using the particle mass, the momentum of the beam could be calculated with a precision of about 0.5%.

C_1 and C_2 were 5 m long threshold Čerenkov counters with spherical mirrors and a single photomultiplier, providing a resolution $\Delta\beta = 6.5 \times 10^{-6}$ (where $\Delta\beta$ is defined as the width in β from threshold to 63% efficiency). The counter efficiency on the plateau was better than 99.99%. Nitrogen or helium were the gases used as radiator. The counters could be used in normal threshold mode or in a differential-threshold mode[4]. In the latter case, pulse-height discrimination on the output of the photomultiplier was used to reject large pulses from unwanted particles. The last Čerenkov counter C_3 was 13 m long and used a plane mirror to reflect the Čerenkov light onto a single photomultiplier through a quartz lens[5]. It had a resolution of $\Delta\beta = 7 \times 10^{-6}$.

In addition to the scintillation counters used to define the beam, each of the differential counters was preceded by a ring anticoincidence counter ($\bar{A}_1$ and $\bar{S}_1$). The purpose of these counters was to remove the effects of the halo of particles surrounding the main beam, particularly the production of Čerenkov light in the glass in the vicinity of the photomultipliers.

During the data taking, as many as four independent techniques for the measurement of the composition of the beam were used. The two differential counters, D and Δ, produced independent pressure curves, and two different modes of operation of the threshold counters were employed either using the normal threshold properties of all the counters, or using the counters C_1 and C_2 in the differential-threshold mode.

Typical pressure curves for these four techniques are illustrated in Fig. 2. Figure 2a is a pressure curve of the D counter. Figure 2b is a similar curve using the Δ counter. Figure 2c shows the threshold counter operation. Figure 2d shows the data obtained using the counters C_1 and C_2 in their differential-threshold mode (denoted by C_1^* and C_2^*). $\bar{C}_3$ was used to veto the lighter particles when K^- or $\bar{p}$ were detected. The clean separation demonstrated by these curves shows that the identification of π^-, K, and $\bar{p}$ up to a momentum of 60 GeV/c can be achieved with only Čerenkov counter techniques.

From pressure curves such as those shown in Fig. 2 the ratios of particles reaching the final scintillation counter could be immediately derived. The particle ratios are directly proportional to the ratios of the areas of the peaks in the pressure curves of the differential Čerenkov counters, since the momentum dispersion in angle was negligible. For the threshold counter data, the particle ratios were derived from the steps in the curves at the particle thresholds. The particle ratios at the production target were obtained by correcting for decay and absorption. The data obtained by the methods described previously agree within the estimated errors, and the final results quoted are a weighted average of these data.

Table 1 shows the experimental results on the particle ratios. Some additional measurements made with the accelerator operating at 43 GeV and 20 GeV are included. The errors represent standard deviations; they are between 5 and 10%. The smaller error of 5% was estimated on the basis of the consistency and reproducibility of the data, as well as on the uncertainty in the absorption corrections.

Figure 3a shows the measured particle ratios, as a function of the laboratory secondary momentum, from 70 GeV protons interacting in aluminium. The lines are hand-drawn and serve mainly to guide the eye. Figure 3b shows the same data together with results from previous measurements[1e]; the variable of the abscissa P/P_{max} is the beam momentum divided by the maximum momentum

the heavier particle may carry (K^- or $\bar{p}$), assuming the usual conservation laws of charge, baryons, and strangeness. This was done to facilitate the comparison of data at quite different incident energies.

The following qualitative statements may be made on the results of particle ratios in the higher momentum region of the spectrum: a) the ratios are strongly decreasing with increasing momentum (about two orders of magnitude over a 20 GeV/c interval); b) over the small angular region studied, the particle ratios appear to be independent of angle; c) when plotted as a function of P/P_{max}, the particle ratios from 70 GeV interactions are similar to those measured at 19.2 GeV/c, near to the maximum momentum, but begin to show an excess when $P/P_{max} \lesssim 0.6$.

Two methods were used to normalize the flux of secondaries. The first was a measurement of the secondary beam rate normalized to 10^{12} circulating protons as indicated by the internal beam monitor of the synchrotron. The standard collimator size*) for this measurement was 4×4 cm^2 (corresponding to $\Delta\Omega = 8 \times 10^{-6}$ sr from target 2) and the momentum slit K_3 was set to ±6mm corresponding to ±1% for $\Delta P/P$. In the second method an absolute calibration giving a cross section scale was obtained from measurements of the Na^{22} produced in the aluminium targets 1 and 3 when exposed to the internal beam for controlled periods. The activation cross section was assumed to remain constant from 28 to 70 GeV, and a value of 10 mb [6] was used. This method provided an absolute calibration of the two monitors F and P when using targets 1 and 3. The normalization of the monitors for target 2 was obtained by interpolation. This procedure gave consistency between measured cross sections at the same momentum from different targets. A final check on this procedure was that the data

*) The maximum flux available when K_1 and K_2 were fully open was ~2.5 times higher than the flux into the standard collimator. The momentum acceptance could be increased to give an increase of ~5 in beam intensity.

normalized by the first method had the same momentum dependence as the results using the Na^{22} normalization of the F monitor. Comparison of the absolute scale of each of these two methods yielded a target efficiency of about 40% .

The resulting laboratory double differential cross sections for pion production from aluminium are tabulated in Table 1. Figure 4 displays the spectra for π^-, K^-, and $\bar{p}$. The scale on the left gives the differential cross section per aluminium nucleus, whilst the scale on the right gives the flux in number of particles per 10^{12} circulating protons into a solid angle $\Delta\Omega = 8 \times 10^{-6}$ sr and a momentum bite $\Delta P = 1$ GeV/c. A large error of ±50% has been assigned to the absolute cross sections because of possible systematic error in the normalization described above.

The data of this experiment permit some additional conclusions to be drawn. When the Čerenkov counters were sensitive to the mass range between K^- and $\bar{p}$, a very low counting rate was observed which precludes the existence in the beam of new particles in this mass range to a level of 10^{-7} of the pion flux. Some of the pressure curves of Fig. 2 were extended to cover the mass range higher than that of the antiproton. In measurements at 40 and 50 GeV/c no counts were recorded, thus placing the following upper limits:

a) no new structure from long-lived particles with mass up to 2.2 GeV to a level of 10^{-6} times the pion fluxes at 40 and 50 GeV/c;

b) antideuteron production is smaller than 10^{-7} times the pion production (3 standard deviation limits).

During the run at 45 GeV/c, a 1.5 m iron absorber was placed behind counter S_5 . A 40 cm diameter counter, S_6 , positioned behind this iron shield was placed in coincidence with the threshold counter combination $(C_1 + C_2)$, and a pressure curve covering the μ^- and π^- thresholds was made. From this measurement it was established that muon content in the 45 GeV/c beam was (0.52 ± 0.07)% .

In conclusion, measurements have been made of the relative particle abundances and fluxes produced in a high momentum negative beam from 70 GeV proton-aluminium interactions. The identification of π^-, K^-, and $\bar{p}$ up to 60 GeV/c required only established Čerenkov counter techniques and did not pose major technical problems. Relative particle abundances are shown to be essentially independent of production angle near the forward direction. The variable P/P_{max} seems to be a useful variable to extrapolate the particle ratios to higher energies, at least near the upper ends of the momentum spectra.

The absolute production cross sections measured in this experiment can be evaluated from Table 1 and are plotted in Fig. 4. The π^- production is approximately in agreement with the prediction of the model of Hagedorn and Ranft[7], but the K^- and $\bar{p}$ are much less abundant than predicted by this model.

The realization of this experiment resulted from the cooperation of many people who ensured the successful operation of the accelerator and of the secondary beam channel and who constructed skilfully much of the experimental equipment. The authors gratefully acknowledge the support of Professors A.A. Logunov, R.M. Sulaev and A.A. Naumov. The CERN part of the group would like to express their thanks to the Directorate of IHEP for their hospitality and acknowledge the invaluable technical assistance of Mr. E. Leya during the installation of their equipment at IHEP.

Table 1

Particle ratios and π^- production cross sections as a function of secondary momentum (P) and production angle (Θ) for several incident proton energies (E_0). All quantities are in the laboratory system.

E_0 (GeV)	P (GeV/c)	(Θ) (mrad)	K^-/π^- (10^{-2})	$\bar{p}/\pi^-$ (10^{-3})	$\frac{d^2\sigma}{d\omega dp}(\pi^-)$ (mb/sr.GeV/c per Al nucleus)
20.1	11.4	12	1.7 ± 0.1	0.53 ± 0.07	
43.1	24.6	0	2.6 ± 0.1	2.1 ± 0.1	
	30.7	0	0.89 ± 0.03	0.28 ± 0.02	
70.0	40.5	0	3.1 ± 0.1	2.50 ± 0.15	53
	40.1	12	3.4 ± 0.1	2.90 ± 0.15	20
	45.3	5	2.4 ± 0.1	1.31 ± 0.07	18
	45.3	15	2.1 ± 0.1	1.46 ± 0.07	4.0
	47.0	3	1.8 ± 0.2	1.10 ± 0.10	
	50.0	0	1.15 ± 0.06	0.49 ± 0.03	12
	50.0	8			3.3
	50.1	10	1.11 ± 0.06	0.50 ± 0.03	2.6
	55.0	4	0.36 ± 0.03	0.09 ± 0.01	2.9
	60.0	0	0.080 ± 0.006	0.011 ± 0.003	1.0
	60.0	3			0.80
	60.0	8			0.10
	63.0	2			0.37
	63.0	6			0.06
	66.0	0			0.11
	66.0	4			0.026
	69.0	2			0.003
	69.0	4			0.001

Error ± 50% for ≥ 1 and < 1

REFERENCES

1. (a) W.F. Baker, R.L. Cool, E.W. Jenkins, T.F. Kycia, S.J. Lindenbaum, W.A. Love, D. Lüers, J.A. Niederer, S. Ozaki, A.L. Read, J.J. Russell, and L.C. Yuan, Phys.Rev.Letters 7, 101 (1961).

   (b) D. Dekkers, J.A. Geibel, R. Mermod, G. Weber, T.R. Willitts, K. Winter, B. Jordan, M. Vivargent, N.M. King, and E.J.N. Wilson, Phys.Rev. 137 B, 962 (1965).

   (c) R.A. Lundy, T.B. Novey, D.D. Yovanovitch and V.L. Telegdi, Phys.Rev.Letters 14, 504 (1965).

   (d) E.W. Anderson, E.J. Bleser, G.B. Collins, T. Fujii, J. Menes, F. Turkot, R.A. Carrigan, R.M. Edelstein, N.C. Hien, T.J. McMahon, and I. Nadelhaft, Phys.Rev.Letters 19, 198 (1968).

   (e) J.V. Allaby, F. Binon, A.N. Diddens, P. Duteil, A. Klovning, R. Meunier, J.P. Peigneux, E.J. Sacharidis, K. Schlüpmann, M. Spighel, J.-P. Stroot, A.M. Thorndike and A.M. Wetherell, paper submitted to the 14th Int.Conf. on High-Energy Physics, Vienna (1968), (CERN, Geneva, 1968).

2. (a) P. Duteil, L. Gilly, R. Meunier, J.P. Stroot, and M. Spighel, Rev.Sci.Instrum. 35, 1523 (1964).

   (b) V.P. Zrelov, "Vavilov-Čerenkov Radiation", Vol. 2, pp.179-180, Atomizdat, Moscow (1968).

3. P. Duteil, J.P. Garron, R. Meunier, J.-P. Stroot, and M. Spighel, CERN 68-14 (1968).

4. Yu.D. Prokoshkin, IHEP preprint 69-7 (1969).

5. S.V. Donskov, V.A. Kachanov, V.M. Kutyin, A.I. Petrukhin, Yu.D. Prokoshkin, E.A. Razuvaev, and R.S. Shuvalov, IHEP preprint 68-16 K (1968).

6. J.B. Cumming, Ann.Rev.Nucl.Science 13, 261 (1963).

7. R. Hagedorn, and J. Ranft, Suppl.Nuovo Cimento 6, 169 (1968) and private communication.

FIGURE CAPTIONS

Fig. 1 Layout of the beam. 1, 2, 3 indicate the positions of the internal aluminium targets. K_1, K_2, and K_3 are collimators; $L_1 - L_{10}$ are quadrupole lenses, $M_1 - M_3$ bending magnets. D, Δ indicate differential Čerenkov counters, $C_1 - C_3$ threshold Čerenkov counters. The scintillation counters $A_1 - A_4$ were used in conjunction with D, $S_1 - S_5$ in conjunction with Δ and $C_1 - C_3$. Scintillation counter S_6, placed after the iron absorber, was used to measure the muon contamination of the beam. P_{123} and F_{1234} are monitor telescopes.

Fig. 2 Pressure curves at different momenta obtained with a) the D counter, b) the Δ counter, c) the threshold counter combination $\bar{C}_1 C_2 \bar{C}_3$, and d) the differential-threshold combination $C_1^* C_2^* \bar{C}_3$.

Fig. 3 a) Particle ratios R measured in this experiment at 70 GeV incident energy, versus beam laboratory momentum P.
b) Particle ratios R versus beam laboratory momentum divided by the kinematically allowed maximum momentum of the heavier particle (K^- and $\bar{p}$, respectively). The broken line represents the 19.2 GeV/c CERN data[1e] for p-p collisions, and coincides with the dependence found by the same group for p-Al collisions (unpublished).

Fig. 4 Laboratory spectra for π^-, K^-, and $\bar{p}$ produced in 70 GeV/c proton-aluminium interactions. The left-hand scale gives the double differential cross section per aluminium nucleus; the right-hand scale gives the flux per 10^{12} circulating protons into a momentum band of $\Delta P = 1$ GeV/c and a collimator 4 × 4 cm (solid angle $\Delta\Omega = 8 \times 10^{-6}$ sr). The lines are interpolated values for the spectra at 0 mrad. The solid points are for $\Theta < 5$ mrad, the open points are in the range $5 < \Theta < 15$ mrad. The exact production angles are given in Table 1.

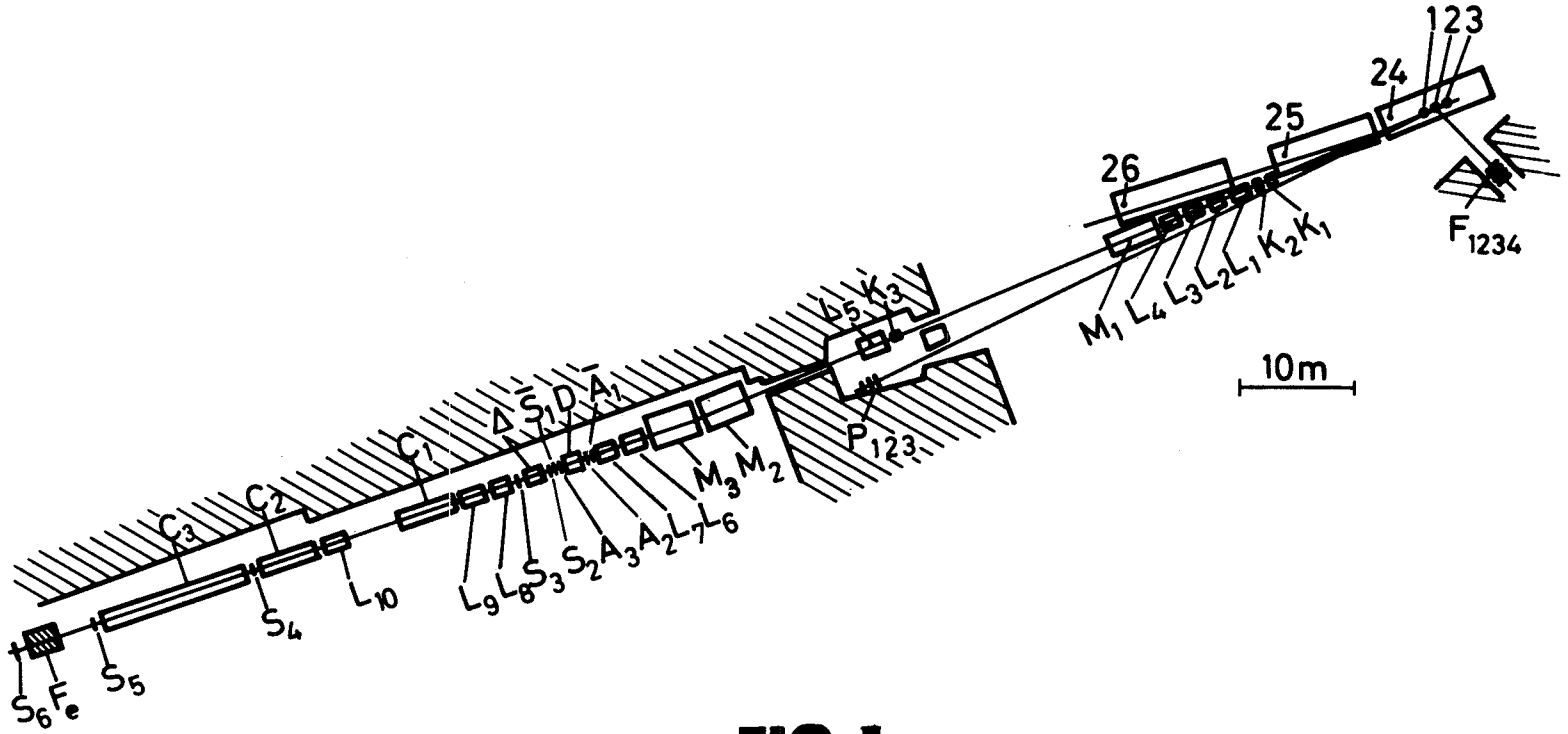
123
24
25
26
F1234
K2 K1
L3 L2 L1
M1 L4
L5 K3
10m
Δ S1 D A1
C1
C3 C2
M3 M2
P123
L9 L8 S3 S2 A3 A2 L7 L6
L10
S4
S5
S6 Fe

FIG 1

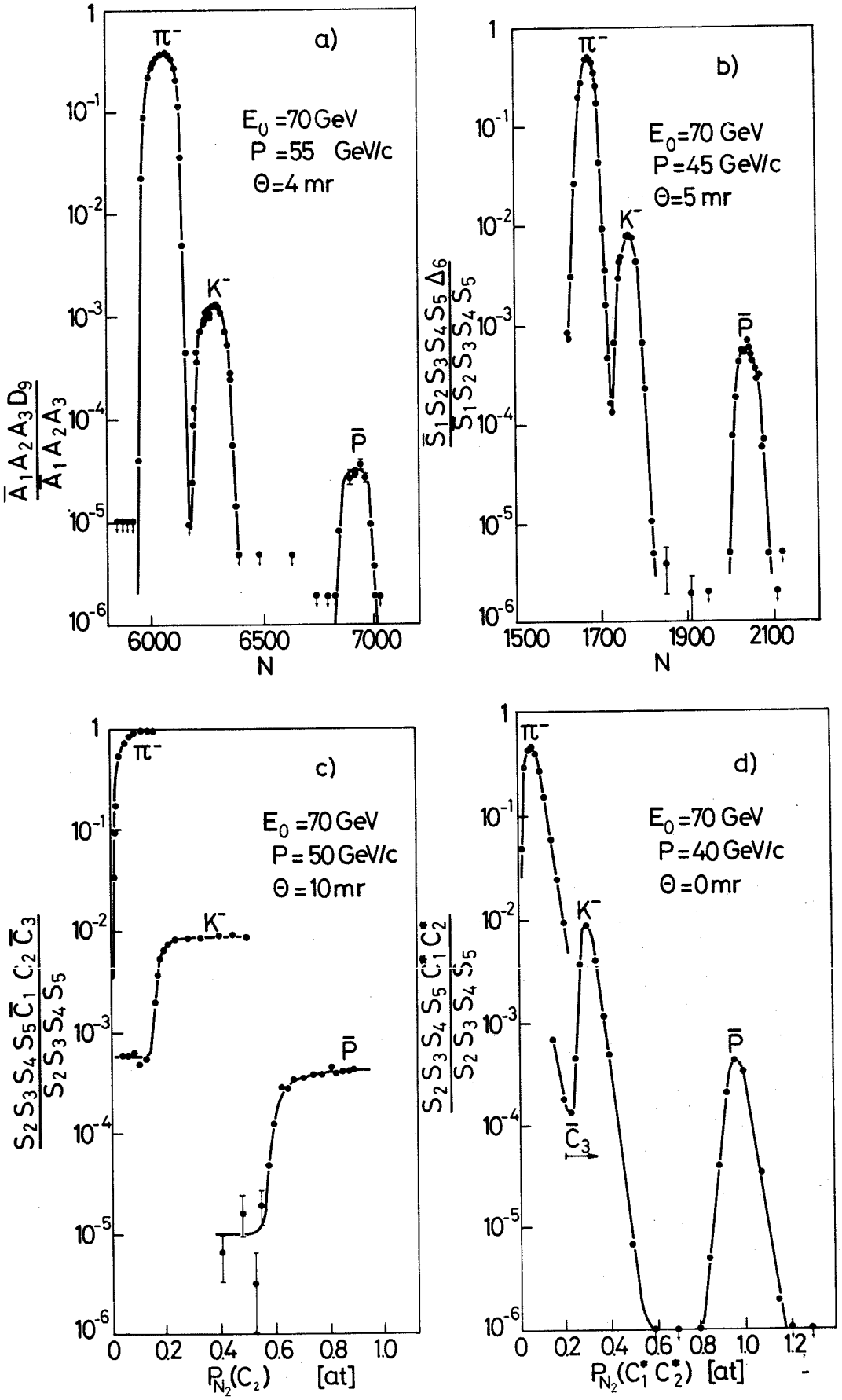
a)
E_0 =70 GeV
P =55 GeV/c
Θ=4 mr
π^-
K^-
$\bar{p}$
$\frac{\bar{A}_1 A_2 A_3 D_9}{A_1 A_2 A_3}$
N
b)
E_0=70 GeV
P=45 GeV/c
Θ=5 mr
$\frac{\bar{S}_1 S_2 S_3 S_4 S_5 \Delta_6}{S_1 S_2 S_3 S_4 S_5}$
c)
E_0 =70 GeV
P = 50 GeV/c
Θ = 10 mr
$\frac{S_2 S_3 S_4 S_5 \bar{C}_1 C_2 \bar{C}_3}{S_2 S_3 S_4 S_5}$
$P_{N_2}(C_2)$ [at]
d)
E_0 =70 GeV
P = 40 GeV/c
Θ = 0 mr
$\bar{C}_3$
$\frac{S_2 S_3 S_4 S_5 C_1^* C_2^*}{S_2 S_3 S_4 S_5}$
$P_{N_2}(C_1^* C_2^*)$ [at]

FIG. 2

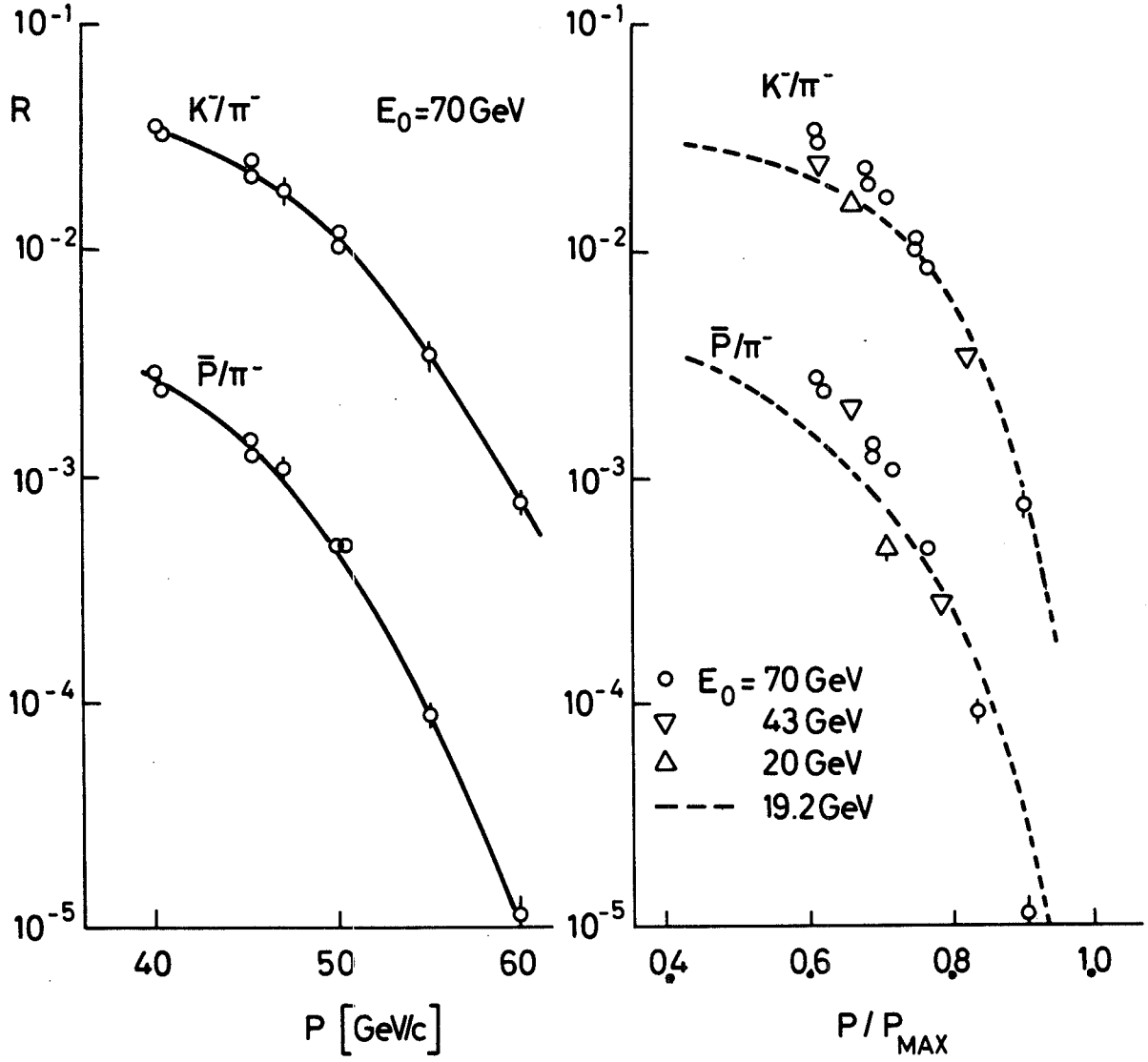
R
10^{-1}
10^{-2}
10^{-3}
10^{-4}
10^{-5}
K^-/π^-
E_0=70 GeV
$\bar{P}/\pi^-$
40
50
60
P [GeV/c]
K^-/π^-
$\bar{P}/\pi^-$
E_0 = 70 GeV
43 GeV
20 GeV
19.2 GeV
0.4
0.6
0.8
1.0
P / P_{MAX}

FIG 3

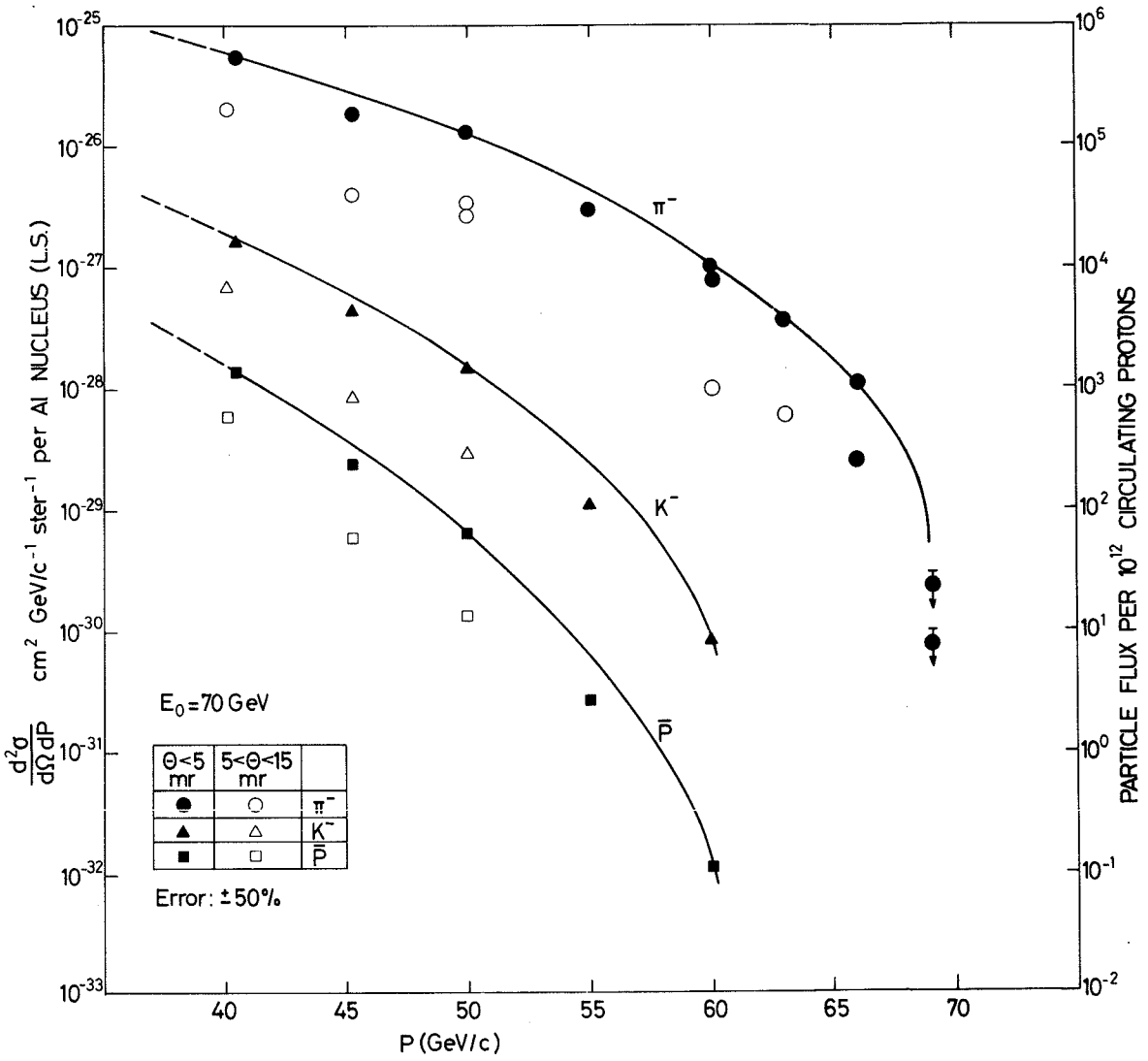
10^{-25}
10^{-26}
10^{-27}
10^{-28}
10^{-29}
10^{-30}
10^{-31}
10^{-32}
10^{-33}
10^{6}
10^{5}
10^{4}
10^{3}
10^{2}
10^{1}
10^{0}
10^{-1}
10^{-2}
40
45
50
55
60
65
70
P (GeV/c)
$\frac{d^2\sigma}{d\Omega dP}$ cm^2 GeV/c^{-1} ster^{-1} per Al NUCLEUS (L.S.)
PARTICLE FLUX PER 10^{12} CIRCULATING PROTONS
π^-
K^-
$\bar{P}$
$E_0 = 70$ GeV
Θ<5 mr
5<Θ<15 mr
π^-
K^-
$\bar{P}$
Error: ±50%

FIG 4